

## Supporting information

### **Manipulating anion intercalation into layered double hydroxide for alkaline seawater oxidation at high current density†**

*Yuwen Wu,<sup>1</sup> Mingpeng Chen,<sup>1, \*</sup> Huachuan Sun,<sup>1</sup> Guohao Na,<sup>1</sup> Dequan Li,<sup>1</sup> Boxue Wang,<sup>1</sup> Yun Chen,<sup>1</sup> Tong Zhou,<sup>1</sup> Jianhong Zhao,<sup>1</sup> Yumin Zhang,<sup>1</sup> Jin Zhang,<sup>1</sup> Feng Liu,<sup>2</sup> Hao Cui,<sup>2</sup> and Qingju Liu<sup>1, \*</sup>*

<sup>1</sup> Yunnan Key Laboratory for Micro/Nano Materials & Technology, National Center for International Research on Photoelectric and Energy Materials, School of Materials and Energy, Yunnan University, Kunming, 650091, China

<sup>2</sup> Yunnan Precious Metals Laboratory Co., Ltd., Kunming, 650106, China

\* Corresponding authors.

Mingpeng Chen: mpchen@ynu.edu.cn (email)

Qingju Liu: qjliu@ynu.edu.cn (email)

<b>Experimental</b> .....	3
<b>Fig. S1.</b> The digital photographs of NiFe LDH-CO <sub>3</sub> <sup>2-</sup> , NiFe LDH-F <sup>-</sup> , NiFe LDH-Cl <sup>-</sup> .....	4
<b>Fig. S2.</b> Morphological characteristics of NiFe LDH on NF at low magnification: (a, b) NiFe LDH-CO <sub>3</sub> <sup>2-</sup> , (c, d) NiFe LDH-F <sup>-</sup> , (e, f) NiFe LDH-Cl <sup>-</sup> .....	5
<b>Fig. S3.</b> a) TEM, b) HRTEM, and c) elemental mapping images of pristine NiFe LDH.....	6
<b>Fig. S4.</b> XRD patterns of the pristine NiFe LDH. ....	7
<b>Fig. S5.</b> High-resolution XPS spectra of (a) Ni 2p (b) Fe 2p (c) O 1s for pristine NiFe LDH.....	8
<b>Fig. S6.</b> F 1s XPS spectra for NiFe LDH-F <sup>-</sup> .....	9
<b>Fig. S7.</b> C 1s XPS spectra for NiFe LDH-CO <sub>3</sub> <sup>2-</sup> .....	10
<b>Fig. S8.</b> Tafel plots of NiFe LDH-A (A=CO <sub>3</sub> <sup>2-</sup> , F <sup>-</sup> , Cl <sup>-</sup> ). ....	11
<b>Fig. S9.</b> Nyquist plots of of NiFe LDH-A (A=CO <sub>3</sub> <sup>2-</sup> , F <sup>-</sup> , Cl <sup>-</sup> ).....	12
<b>Fig. S10.</b> CV curves in the non-Faradaic region (0.1~0.2 V vs Hg/HgO) with various scan rates (20-100 mV s <sup>-1</sup> ) for (a) NiFe LDH-CO <sub>3</sub> <sup>2-</sup> , (b) NiFe LDH-F <sup>-</sup> , (c) NiFe LDH-Cl <sup>-</sup> .....	13
<b>Table S1.</b> Comparison of representative OER in alkaline simulated seawater or alkaline seawater. ....	14
<b>Fig. S11.</b> XRD patterns of NiFe LDH-Cl <sup>-</sup> before and after OER test. ....	16
<b>Fig. S12.</b> EDS elemental mapping images of NiFe-LDH-Cl <sup>-</sup> after OER test.....	17
<b>Fig. S13.</b> (a) TEM and (b) HRTEM images of NiFe LDH-Cl <sup>-</sup> after OER test..	18
<b>Fig. S14.</b> (a) Ni 2p, (b) Fe 2p, (c) O 1s, and (d) Cl 2p XPS spectra of NiFe LDH-Cl <sup>-</sup> before and after OER test. ....	19

## Experimental

### 1.1 Synthesis of NiFe LDH-CO<sub>3</sub><sup>2-</sup>, NiFe LDH-F<sup>-</sup>, and NiFe LDH-Cl<sup>-</sup>

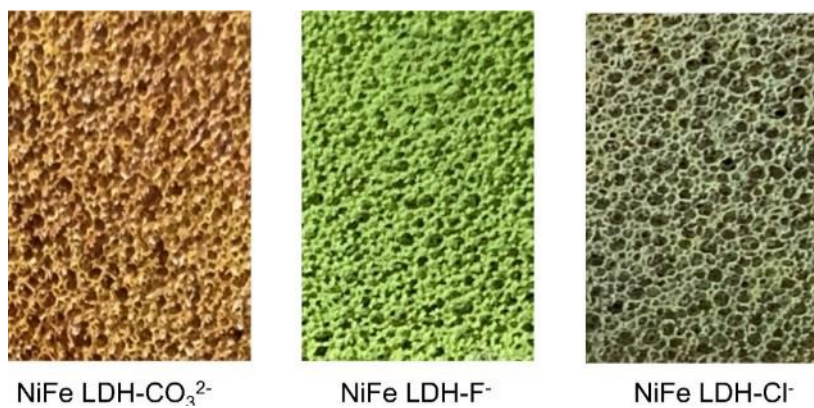
1 mmol Ni(NO<sub>3</sub>)<sub>2</sub>·6H<sub>2</sub>O and 1 mmol Fe(NO<sub>3</sub>)<sub>3</sub>·9H<sub>2</sub>O were dissolved in 35 mL of deionized (DI) water, add 10 mmol CO(NH<sub>2</sub>)<sub>2</sub>, NH<sub>4</sub>F, and NaCl separately, and then the pretreated nickel foam (NF, 2 × 3 cm<sup>2</sup>) was immersed in the solution, and kept at 120 °C for 6 h. After drying in air, nickel foam self-supporting NiFe LDH-CO<sub>3</sub><sup>2-</sup>, NiFe LDH-F<sup>-</sup>, and NiFe LDH-Cl<sup>-</sup> nanosheets were obtained.

### 1.2 Materials characterization

Scanning electron microscopy (SEM, GeminiSEM 460), and transmission electron microscopy (TEM, JEM-2100) were conducted to characterize the morphologies and elements distribution of catalysts. X-ray diffraction (XRD) data was recorded on an X-ray diffractometer (Rigaku TTR-III) with a Cu K $\alpha$  source. X-Ray photoelectron spectroscopy (XPS, K-Alpha) tests were conducted using Al source radiation.

### 1.3. Electrochemical measurements

An EnergyLab XM potentiostat (Solartron Analytical) was utilized for electrochemical measurements in a conventional three-electrode system. The working electrode, reference electrode, and counter electrode were the as-synthesized sample, Hg/HgO electrode, and carbon rod, respectively. For uniformity, all measurements were calibrated to the RHE using the formula  $E_{\text{RHE}} = E_{\text{Hg/HgO}} + 0.098 \text{ V} + 0.059 \times \text{pH}$ . Linear sweep voltammetry (LSV) curves with 95% iR compensation were documented at a scan rate of 2 mV s<sup>-1</sup>. The electrochemical double-layer capacitance ( $C_{\text{dl}}$ ) by implementing CV measurements with varying scan rates ranging from 20 to 100 mV/s in the non-faradaic region. The electrochemical impedance spectroscopy (EIS) was performed with a frequency from 100 kHz to 0.01 Hz.



NiFe LDH-CO<sub>3</sub><sup>2-</sup>

NiFe LDH-F<sup>-</sup>

NiFe LDH-Cl<sup>-</sup>

**Fig. S1.** The digital photographs of NiFe LDH-CO<sub>3</sub><sup>2-</sup>, NiFe LDH-F<sup>-</sup>, NiFe LDH-Cl<sup>-</sup>.

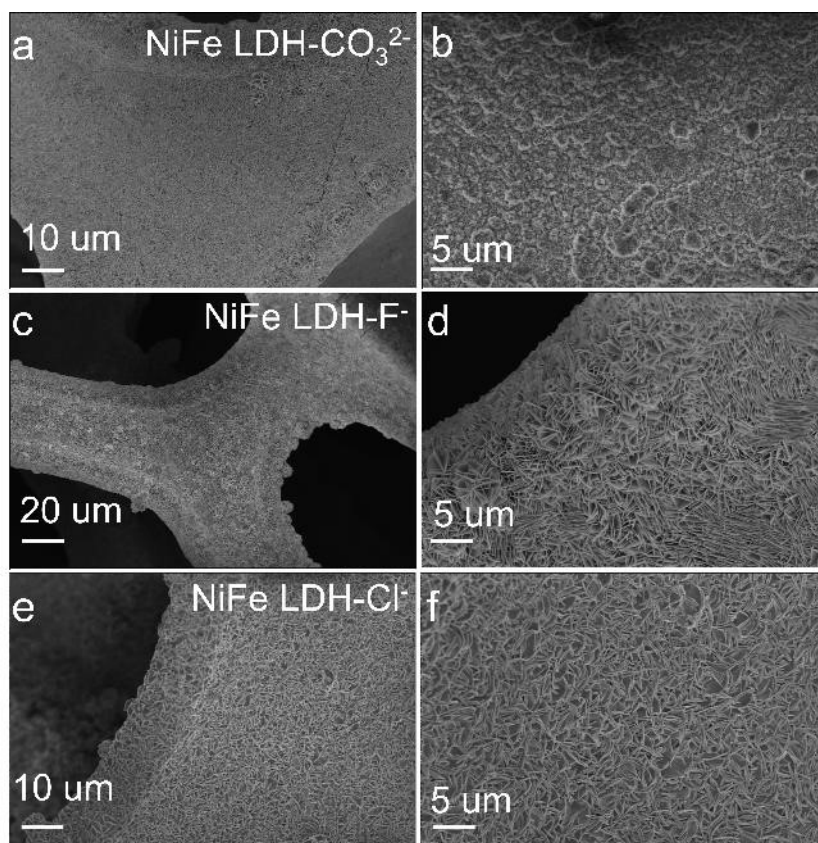


**Fig. S2.** Morphological characteristics of NiFe LDH on NF at low magnification: (a, b) NiFe LDH-CO<sub>3</sub><sup>2-</sup>, (c, d) NiFe LDH-F<sup>-</sup>, (e, f) NiFe LDH-Cl<sup>-</sup>.

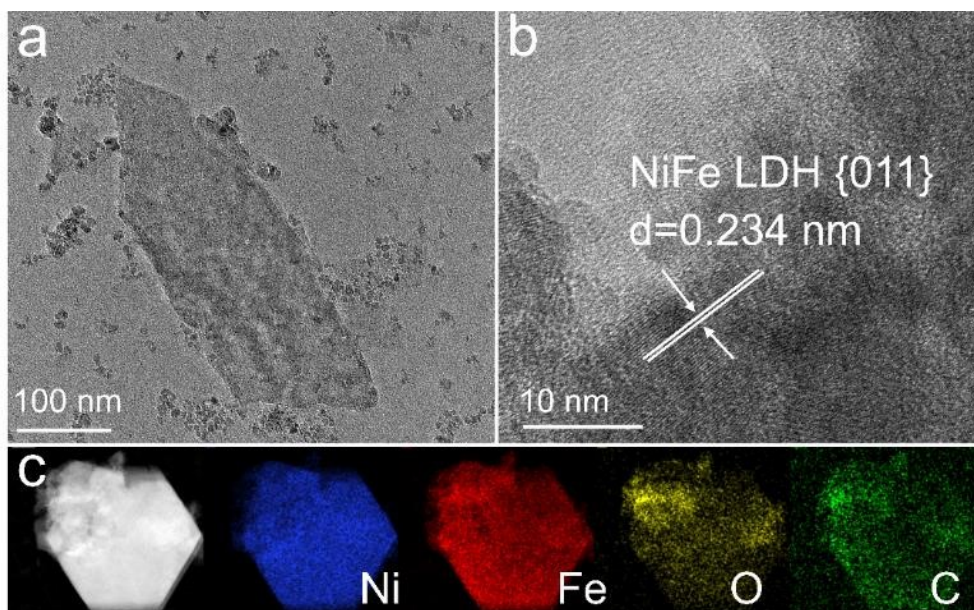


**Fig. S3.** a) TEM, b) HRTEM, and c) elemental mapping images of pristine NiFe LDH.

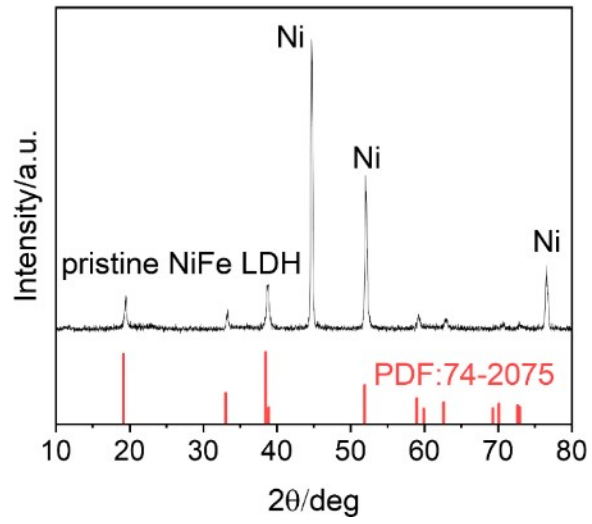


**Fig. S4.** XRD pattern of the pristine NiFe LDH.

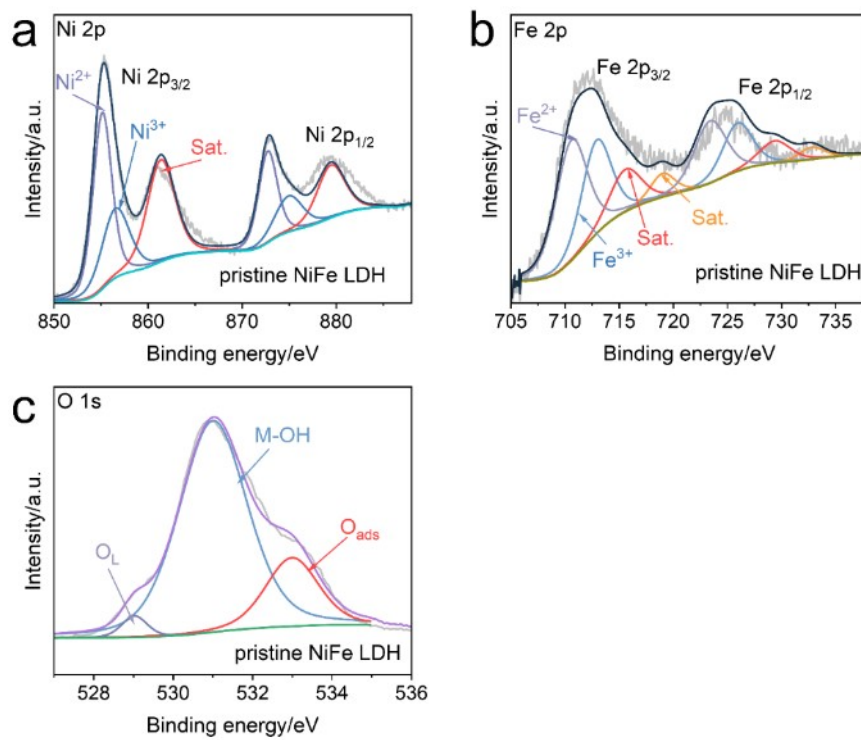


**Fig. S5.** High-resolution XPS spectra of (a) Ni 2p (b) Fe 2p (c) O 1s for pristine NiFe LDH.



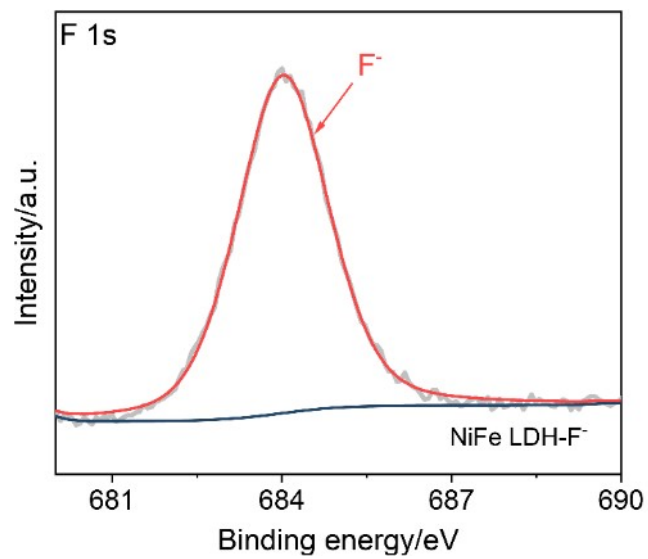


**Fig. S6.** F 1s XPS spectra for NiFe LDH-F<sup>-</sup>.

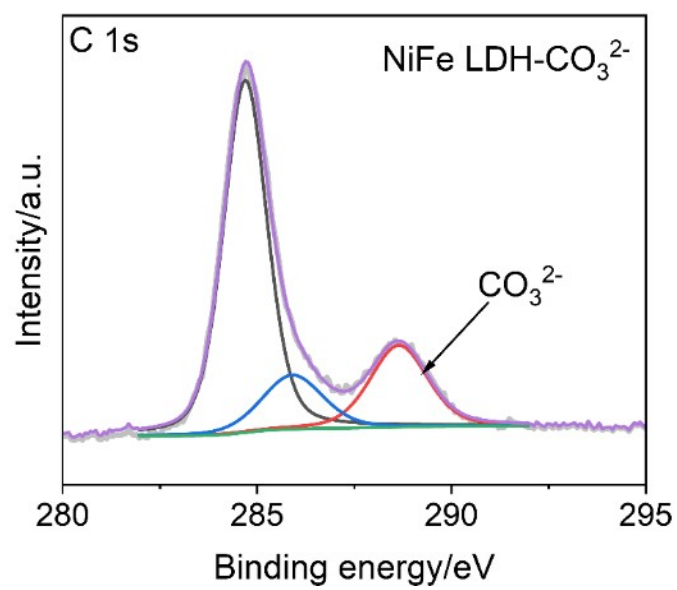


**Fig. S7.** C 1s XPS spectra for NiFe LDH-CO<sub>3</sub><sup>2-</sup>.

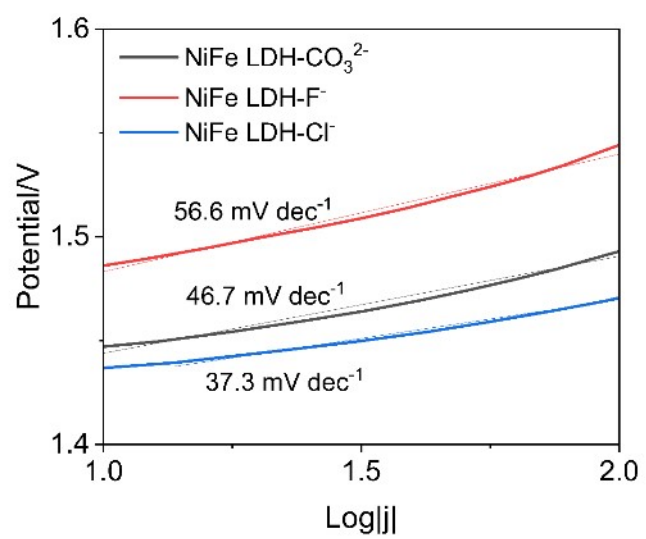


**Fig. S8.** Tafel plots of NiFe LDH-A (A=CO<sub>3</sub><sup>2-</sup>, F<sup>-</sup>, Cl<sup>-</sup>).

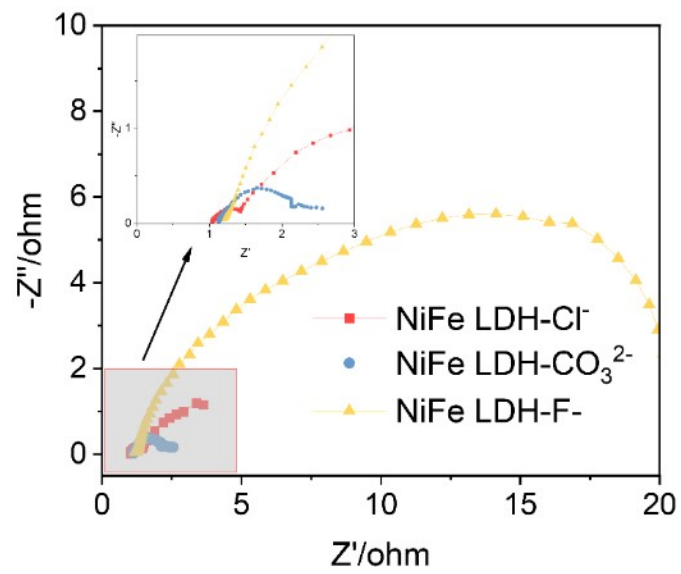


**Fig. S9.** Nyquist plots of of NiFe LDH-A (A=CO<sub>3</sub><sup>2-</sup>, F<sup>-</sup>, Cl<sup>-</sup>).

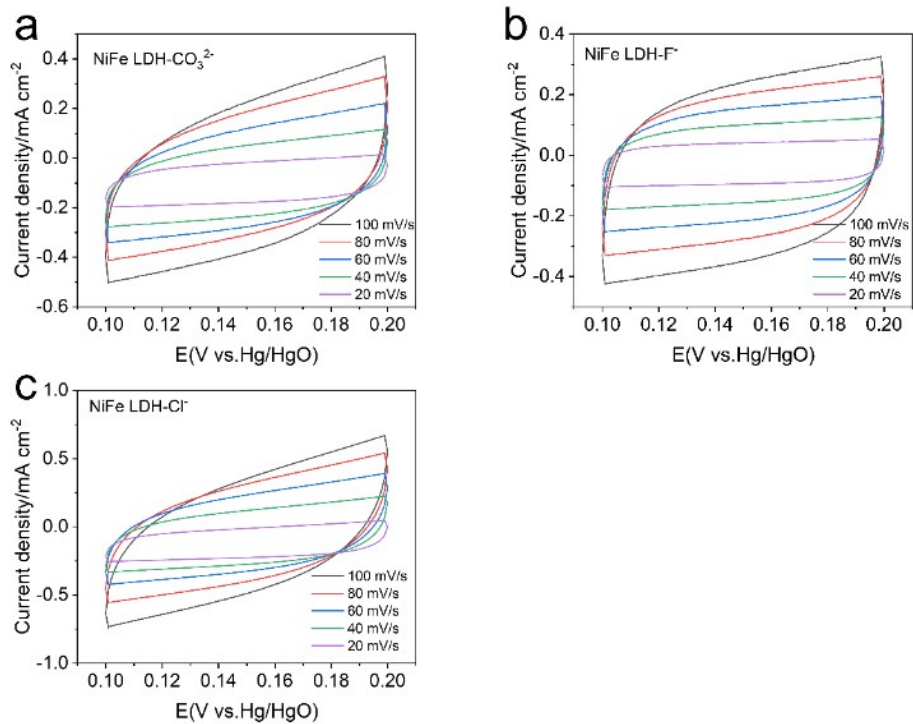


**Fig. S10.** CV curves in the non-Faradaic region (0.1~0.2 V vs Hg/HgO) with various scan rates (20-100 mV s<sup>-1</sup>) for (a) NiFe LDH-CO<sub>3</sub><sup>2-</sup>, (b) NiFe LDH-F<sup>-</sup>, (c) NiFe LDH-Cl<sup>-</sup>.

**Table S1.** Comparison of representative OER in alkaline simulated seawater or alkaline seawater.

Catalyst	j/mA cm <sup>-2</sup>	$\eta$ /mV	Stability/h	Electrolyte	Refs
NiFe LDH(NaCl)	100	240	N/A	1 M KOH	This work
	200	255	200		
	500	300	N/A		
	500	330	N/A	0.5 M NaCl+1 M KOH	
	500	325	N/A	1 M NaCl+1 M KOH	
	500	310	N/A	2 M NaCl+1 M KOH	
	200	350	100	seawater+1 M KOH	
NiFe LDH_CO <sub>3</sub> <sup>2-</sup>	100	237	200	1 M KOH +0.5 M NaCl	1
	200	264			
	500	302			
	1000	351			
	500	N/A	1000	1 M KOH + 0.5 M NaCl + 1 M Na <sub>2</sub> CO <sub>3</sub>	
	1000	N/A			
NiIr-LDH	100	286	N/A	1M KOH + 0.5 M NaCl	2
Fe(OH) <sub>3</sub> -Ni(SO <sub>4</sub> ) <sub>0.3</sub> (OH) <sub>1.4</sub> -Ni(OH) <sub>2</sub>	100	268	N/A	1 M KOH + 0.5 M NaCl	3
	200	283	500		

	400	290	N/A		
CoFe-Ni <sub>2</sub> P	100	246	140	1 M KOH + 0.5 M NaCl	4
	500	360	510	1 M KOH + Seawater	
B- MnFe <sub>2</sub> O <sub>4</sub> @MFOC	100	333	100	1 M KOH + 0.5 M NaCl	5
	500	N/A			
	100	405		1 M KOH + Seawater	
NiTe@FeOOH	100	280	100	Alkaline Seawater	6
	500	328	N/A		
Co <sub>x</sub> P <sub>v</sub> @NC	500	323	N/A	1 M KOH + Seawater	7
	800	N/A	100		
Ni <sub>x</sub> Cr <sub>y</sub> O	100	370	275	1 M KOH + Seawater	8
	500	460	100		
Cr-Co <sub>x</sub> P	100	334	140	1 M KOH + Seawater	9
	500	392	N/A		
	1000	423	N/A		

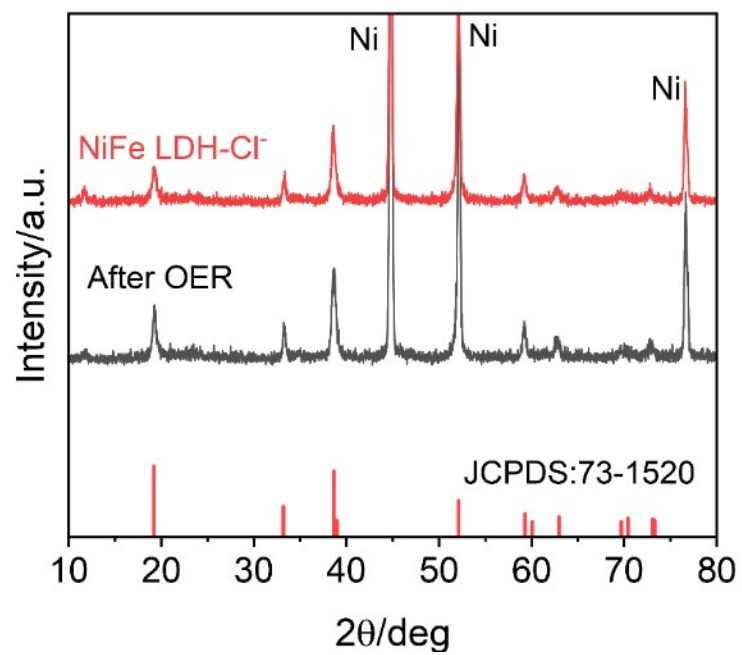


**Fig. S11.** XRD patterns of NiFe LDH-Cl<sup>-</sup> before and after OER test.



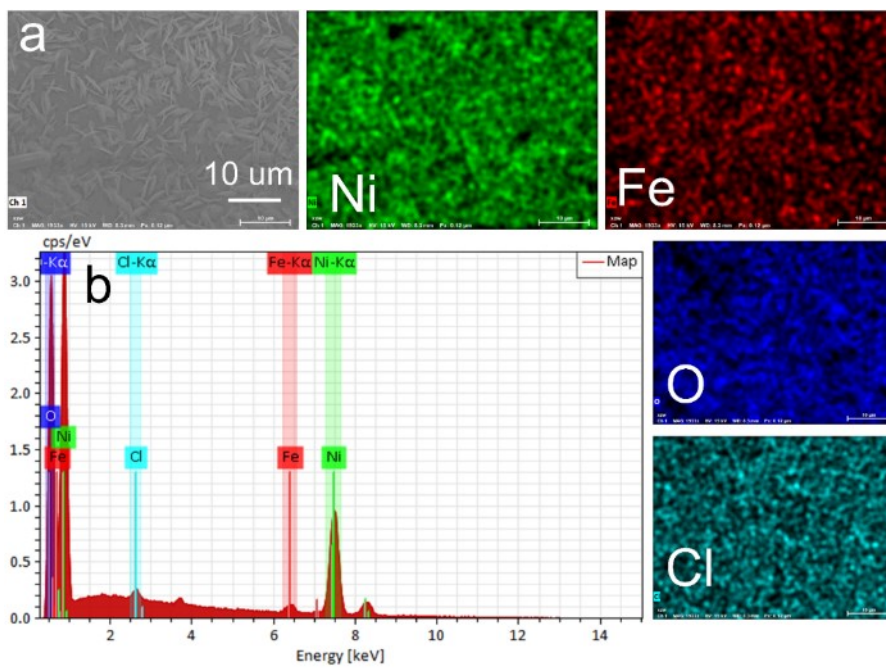


**Fig. S12.** EDS elemental mapping images of NiFe-LDH-Cl<sup>-</sup> after OER test.

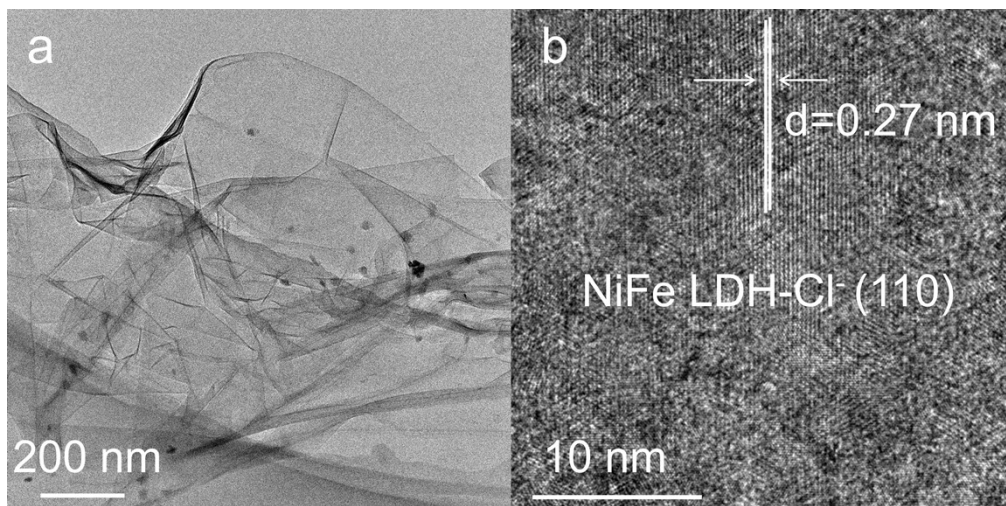


**Fig. S13.** (a) TEM and (b) HRTEM images of NiFe LDH-Cl<sup>-</sup> after OER test.

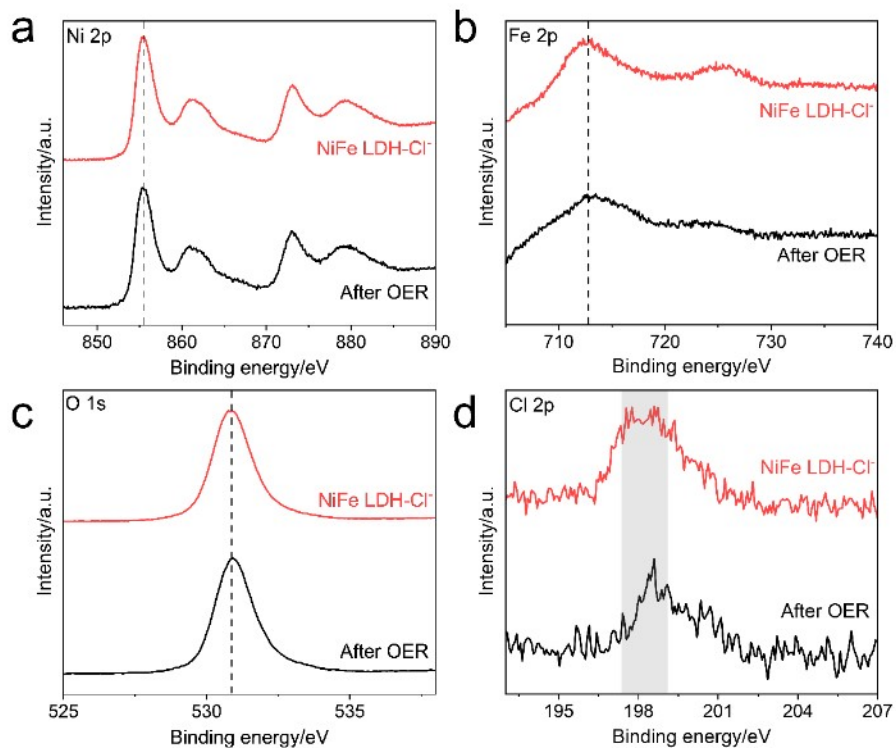


**Fig. S14.** (a) Ni 2p, (b) Fe 2p, (c) O 1s, and (d) Cl 2p XPS spectra of NiFe LDH-Cl before and after OER test.

## References

1. P.-J. Deng, Y. Liu, H. Liu, X. Li, J. Lu, S. Jing and P. Tsiakaras, *Advanced Energy Materials*, 2024, **n/a**, 2400053.
2. H. You, D. Wu, D. Si, M. Cao, F. Sun, H. Zhang, H. Wang, T.-F. Liu and R. Cao, *Journal of the American Chemical Society*, 2022, **144**, 9254-9263.
3. J. Lu, Y. Liu and H.-P. Liang, *Science China Chemistry*, 2024, **67**, 687-695.
4. C. Huang, Q. Zhou, L. Yu, D. Duan, T. Cao, S. Qiu, Z. Wang, J. Guo, Y. Xie, L. Li and Y. Yu, *Advanced Energy Materials*, 2023, **13**, 2301475.
5. M. Chen, N. Kitiphatpiboon, C. Feng, Q. Zhao, A. Abudula, Y. Ma, K. Yan and G. Guan, *Applied Catalysis B: Environmental*, 2023, **330**, 122577.
6. X. Gao, J. Chen, Y. Yu, F. Wang, X. Wu, X. Wang, W. Mao, J. Li, W. Huang, Q. Chen, R. Li, C. You, S. Wang, X. Tian and Z. Kang, *Chemical Engineering Journal*, 2023, **474**, 145568.
7. X. Wang, X. Liu, S. Wu, K. Liu, X. Meng, B. Li, J. Lai, L. Wang and S. Feng, *Nano Energy*, 2023, **109**, 108292.
8. A. Malek, Y. Xue and X. Lu, *Angewandte Chemie International Edition*, 2023, **62**, e202309854.
9. Y. Song, M. Sun, S. Zhang, X. Zhang, P. Yi, J. Liu, B. Huang, M. Huang and L. Zhang, *Advanced Functional Materials*, 2023, **33**, 2214081.